J Neuropathol Exp Neurol
Vol. 72, No. 9
September 2013
pp. 846–860

ORIGINAL ARTICLE

Disruption of CDH2/N-Cadherin–Based Adherens Junctions Leads to Apoptosis of Ependymal Cells and Denudation of Brain Ventricular Walls

Cristian Oliver, César A. González, PhD, Genaro Alvial, Carlos A. Flores, PhD, Esteban M. Rodríguez, MD, PhD, and Luis Federico Bátiz, MD, PhD

Abstract

Disruption/denudation of the ependymal lining has been associated with the pathogenesis of various human CNS disorders, including hydrocephalus, spina bifida aperta, and periventricular heterotopia. It has been traditionally considered that ependymal denudation is a consequence of mechanical forces such as ventricular enlargement. New evidence indicates that ependymal disruption can precede ventricular dilation, but the cellular and molecular mechanisms involved in the onset of ependymal denudation are unknown. Here, we present a novel model to study ependymal cell pathophysiology and demonstrate that selective disruption of N-cadherin–based adherens junctions is sufficient to provoke progressive ependymal denudation. Blocking N-cadherin function using specific peptides that interfere with the histidine-alanine-valine extracellular homophilic interaction domain caused early pathologic changes characterized by disruption of zonula adherens and abnormal intracellular accumulation of N-cadherin. These changes then triggered massive apoptosis of ependymal cells and denudation of brain ventricular walls. Because no typical extrinsic mechanical factors such as elevated pressure or stretching forces are involved in this model, the critical role of N-cadherin–based adherens junctions in ependymal survival/physiology is highlighted. Furthermore, the results suggest that abnormal adherens junctions between ependymal cells should be considered as key components of the pathogenesis of CNS disorders associated with ependymal denudation.

From the Instituto de Anatomía, Histología y Patología, Facultad de Medicina, Universidad Austral de Chile, Valdivia, Chile (CO, CAG, GA, EMR, LFB); Mitchell Center for Alzheimer's Disease and Related Brain Disorders, Department of Neurology, University of Texas Houston Medical School, Houston, Texas (CAG); and Centro de Estudios Científicos, Valdivia, Chile (CAF).

Send correspondence and reprint requests to: Luis Federico Bátiz, MD, PhD, Instituto de Anatomía, Histología y Patología, Facultad de Medicina, Universidad Austral de Chile. Valdivia, Chile; E-mail: federicobatiz@uach.cl

This work was funded by the Chilean National Commission for Scientific & Technological Research (CONICYT) (Fondecyt 1070241 and 1111018 to Esteban Rodríguez; Fondecyt 11100408 and Base Financing Program to Carlos Flores; Fondecyt 11090373 to Luis Bátiz) and the I + D Office at Universidad Austral de Chile (DID-UACh).

The authors declare that they have no competing interests.

Supplemental digital content is available for this article. Direct URL citations appear in the printed text and are provided in the HTML and PDF versions of this article on the journal's Web site (www.jneuropath.com).

Key Words: Adherens junctions, Apoptosis, CDH2/N-cadherin, Ependymal cells, Ependymal disruption/denudation, Hydrocephalus, Periventricular heterotopia.

INTRODUCTION

The ventricular surface of the CNS of adult mammals is lined by several lineages of ependymal cells, some of which are located at specific and discrete regions (1–4). During development, most ependymal cells originate from radial glial cells before birth (5), but ependymal cells are born postnatally in some mouse brain regions (6). Ependymal cells have barrier and signaling functions between cerebrospinal fluid and neural tissue (7, 8). A function common to all types of multiciliated ependymal cells is the coordinated beating of cilia that is responsible for laminar cerebrospinal fluid flow (9, 10). Indeed, several strains of mice with targeted or spontaneous mutations in cilia proteins develop hydrocephalus (9, 11–13). We have also previously demonstrated that the loss of ependymal cells (denudation) leads to cerebral aqueduct obliteration and severe hydrocephalus in hyh mutant mice (4, 14). Similarly, ependymal denudation has been considered to be a primary neuropathologic event involved in the onset of various human CNS disorders, including communicating hydrocephalus (15), spina bifida aperta (SBA) (16), and periventricular heterotopia (17). Although ependymal denudation seems to be a key pathogenic mechanism in hydrocephalus and other CNS conditions, the cellular and molecular mechanisms leading to this phenomenon are virtually unknown.

Different reports suggest that ependymal cells are devoid of functional tight junctions (TJs) and that they are joined together only by adherens and gap junctions (8, 18, 19). In this context, defects in junction proteins and junction complexes seem to be good candidates for involvement in the disassembling and disruption of the ependymal lining. Indeed, adherens junctions are thought to play an important role in the stability of neuroepithelial and radial glial cells (20, 21). Furthermore, recent data from our laboratory suggest that abnormal subcellular distribution of N-cadherin, a key component of adherens junctions, precedes ependymal denudation in SBA human fetuses (16). N-cadherin is a transmembrane glycoprotein that is highly expressed in the CNS (22). Like all members of the Type I classic cadherin family, N-cadherin establishes

homophilic calcium-dependent bonds between neighboring cells and forms beltlike adherens junctions (zonula adherens) linked to the actin cytoskeleton (23).

Here, we evaluated the neuropathologic consequences of blocking N-cadherin function in ependymal cells. We developed a novel organotypic culture system from adult bovine collicular recess roof (CRr). This culture system mimics the morphology and functional properties of the multiciliated ependyma in vivo. In this model, ependymal cells were exposed to specific mimetic-blocking peptides directed against a portion of the distalmost N-cadherin ectodomain region, which is critical for cadherin-cadherin homophilic adhesive binding. We analyzed the consequences at different time points and investigated the cellular mechanisms that may precede and be implicated in ependymal denudation after blocking N-cadherin function.

MATERIALS AND METHODS

Organotypic Culture of Adult Bovine CRr

The CR is a dorsal expansion of the middle region of the aqueduct of Sylvius. The CRr is a thin wall formed by multiciliated ependyma and a thin subependymal neuropil. The CRr was selected for organotypic cultures because it has several advantages over some other ventricular regions: 1) it is easily accessible and can be rapidly dissected; 2) the ependymal cells in this region are histologically very homogeneous; 3) the thinness of the tissue in situ reduces the chance of scraping ventricular walls (other regions) and mechanical disruption of the ependyma; and 4) the sheetlike shape of the CRr facilitates manipulation during dissection when the explants are obtained. Samples of adult bovine CRr were obtained from a local slaughterhouse (FRIVAL, Valdivia, Chile) shortly after death (maximum postmortem period ~10–15 minutes). The region corresponding to the mesencephalon was rapidly dissected out and transferred to ice-cold Hanks solution (Sigma-Aldrich, St. Louis, MO). The CRr was dissected out and used to obtain explants of approximately 1 mm^2. Each CRr rendered about 100 explants. The explants were cultured in low-attachment tissue culture plates with fresh DMEM/F12 culture medium (Sigma-Aldrich) supplemented with 10% fetal bovine serum (Sigma-Aldrich) and 2.5% adult bovine serum (Sigma-Aldrich) at 37°C and 5% CO_2. Viability of ependymal cells in CRr explants was confirmed at every experimental period and treatment by directly observing ciliary beating under an inverted phase-contrast microscope. All procedures at the slaughterhouse and at the laboratories were performed in accordance with the national sanitary and animal welfare laws, guidelines, and policies and were revised and approved by the Institutional Bioethics Committee (Universidad Austral de Chile, Valdivia, Chile).

N-Cadherin Function–Blocking Assays

Disruption of cadherin-based junctions by antibodies or synthetic peptides has been previously validated in other tissues and cell systems (24–26). A 16-mer synthetic mimetic peptide (HLRA*HAV*DINGNQVEN) containing the conserved histidine-alanine-valine (HAV) cadherin recognition sequence (the presumptive binding domain of all Type I classic cadherins) was generated with flanking amino acids corresponding to bovine N-cadherin sequence (NCBI Sequence Viewer, USA). Previous studies have shown that the HAV-flanking sequence confers cadherin-type specificity (27, 28). The same peptide sequence has been used previously for functional N-cadherin blocking assays in mice (24), and sequence alignment indicates that the 16 amino acids of the HAV peptide are 100% homologous with mouse sequence (Table, Supplemental Digital Content 1, http://links.lww.com/NEN/A482). A second ''scrambled'' peptide containing the same amino acids as the HAV peptide but in a different sequence (ARLQHDVNANVHEING) was generated for control studies. The scrambled peptide has no known matches (verified using EMBL-EBI FASTA search). Both synthetic peptides were purchased from Invitrogen (Carlsbad, CA).

Groups of explants (~20 explants per group) were cultured for different periods (0, 12, 24, and 36 hours) under 3 different conditions as follows: Experimental: HAV peptide was added to the culture medium at a final concentration of 400 μg/mL; Control 1: ''Scrambled'' peptide was added to the culture medium at a final concentration of 400 μg/mL; Control 2 (no treatment): no peptide was added to the culture medium. The final concentration of peptides was defined based on preliminary experiments in which concentrations of 100, 200, 400, and 600 μg/mL were used at different periods. In these studies, HAV peptide exhibited a maximal effect (i.e. ependymal denudation at 24 hours' treatment) at 400 μg/mL.

Light Microscopy

After each experimental procedure, CRr explants were fixed in Bouin fixative for 24 hours at 4°C. Then, samples were dehydrated and embedded in Paraplast (Sigma-Aldrich). Serial sections (4-μm thick) were obtained and mounted on silanized (3-aminoprohoxysylanepyltrie; Polysciences, Inc., Warrington, PA) slides and used for hematoxylin and eosin staining and immunohistochemistry/immunofluorescence. Samples were visualized using a Zeiss Axioskop Microscope coupled to a digital camera (Axiocam MR, Zeiss).

Immunohistochemistry/Immunofluorescence

Paraffin-embedded sections were processed for immunocytochemistry and immunofluorescence as previously described (4). The following primary antibodies were used: 1) anti–glial fibrillary acidic protein (GFAP), mouse monoclonal (1:1000; Sigma); 2) anti–caveolin-1, rabbit polyclonal (1:200, N-20; Santa Cruz Biotechnology, Santa Cruz, CA); and 3) anti–active-caspase-3, rabbit polyclonal (1:50, G748A; Promega, Madison, WI). All incubations were overnight and at room temperature (RT). Anti-rabbit IgG raised in goat (Sigma) or anti-mouse IgG developed in rabbit (Sigma) were used as secondary antibodies at 1:50 dilution for 1 hour at RT. Immunoreaction was detected using the Elite Vectastain ABC kit (PK-6200; Vector Laboratories, Burlingame, CA). 3,3′-Diaminobenzidine tetrahydrochloride (Sigma) was used as chromogen. For immunofluorescence detection of N-cadherin or active caspase-3, sections were sequentially incubated in the corresponding primary antibodies overnight and in Alexa Fluor 488–conjugated goat anti-rabbit IgG antibody (Invitrogen) for 30 minutes. In some experiments, nuclear counterstaining was performed using TOPRO-3 (Invitrogen) for 5 minutes at

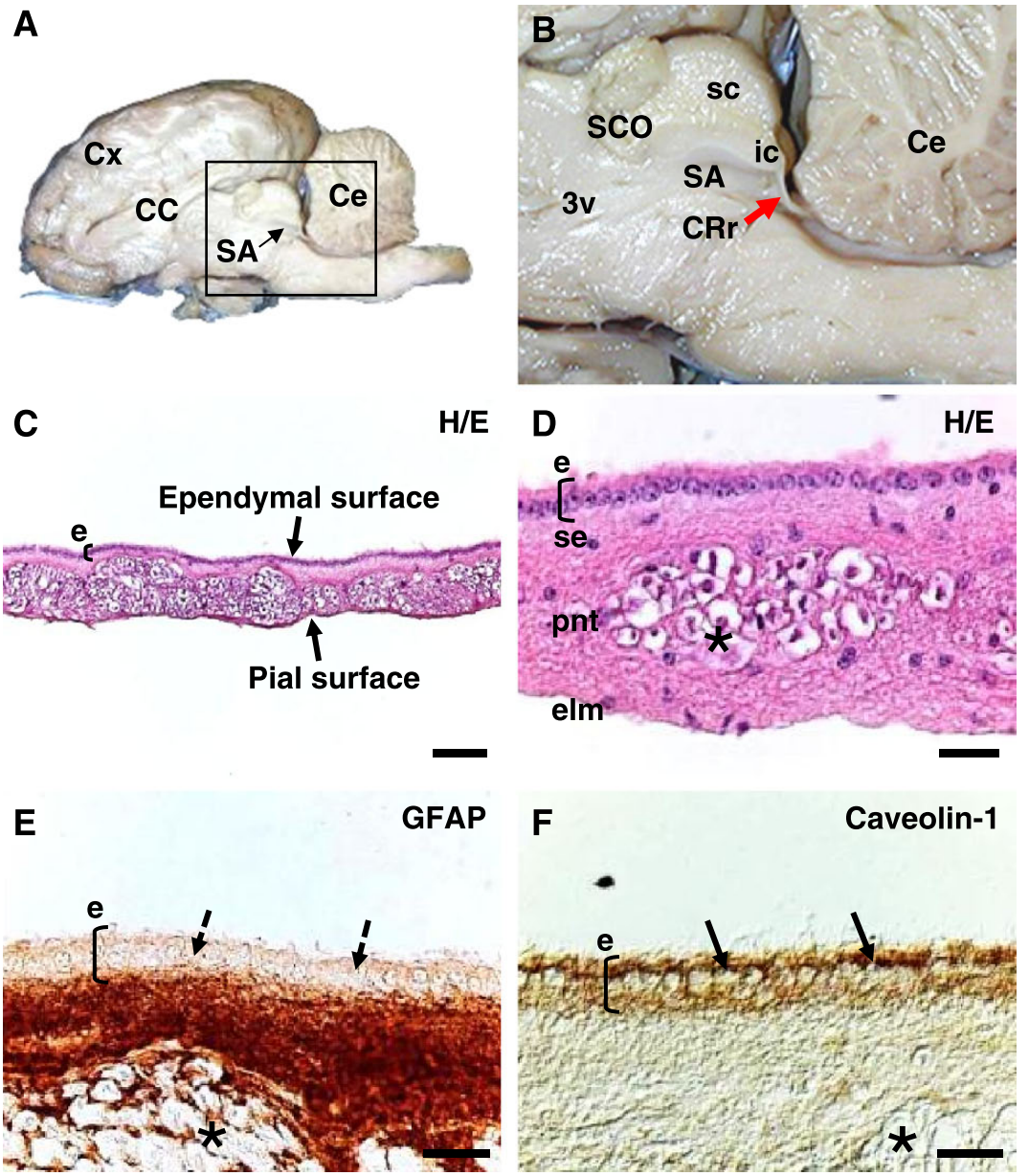

FIGURE 1. Explants from bovine collicular recess roof (CRr). **(A)** View of a midsagittal section of an adult bovine brain showing the region magnified in **(B)** (square). **(B)** Magnification of the mesencephalic region. The red arrow indicates the anatomic position of the CRr. **(C, D)** Explant from bovine CRr stained with hematoxylin and eosin (H/E). The thickness of explants was 157 ± 15.89 μm (n = 30). Different regions are distinguished: ependymal (e), subependymal zone (se), periaqueductal neural tissue (pnt) including numerous axon bundles (asterisk), and external limiting membrane (elm). **(E, F)** Glial fibrillary acidic protein (GFAP) **(E)** and caveolin-1 **(F)** immunostaining of the CRr. Asterisks show axon bundles. The pnt is mainly composed of GFAP-positive astrocytes. Mature multiciliated ependymal cells are GFAP negative (broken arrows in **[E]**) and strongly express caveolin-1 (full arrows in **[F]**). SA, Sylvian aqueduct; 3v, third ventricle; CC, corpus callosum; Ce, cerebellum; Cx, cerebral cortex; ic, inferior colliculus; sc, superior colliculus; SCO, subcommissural organ. Scale bars = **(C)** 100 μm; **(D–F)** 20 μm.

RT. Fluorescence was examined using an inverted Olympus FluoView FV1000 confocal microscope.

Terminal Deoxynucleotidyl Transferase dUTP Nick End Labeling Assay

The colorimetric terminal deoxynucleotidyl transferase dUTP nick end labeling (TUNEL) DeadEnd system (Promega) was used. Briefly, CRr explants were fixed in 4% paraformaldehyde for 2 to 4 hours before being dehydrated and embedded in paraffin using standard histologic methods. Serial sections (4-μm thick) were obtained and mounted on silanized slides. Before hybridization, sections were incubated at 45°C overnight, deparaffinized with xylene, and then rehydrated through an ethanol series to water and pretreated with 20 μg/mL proteinase

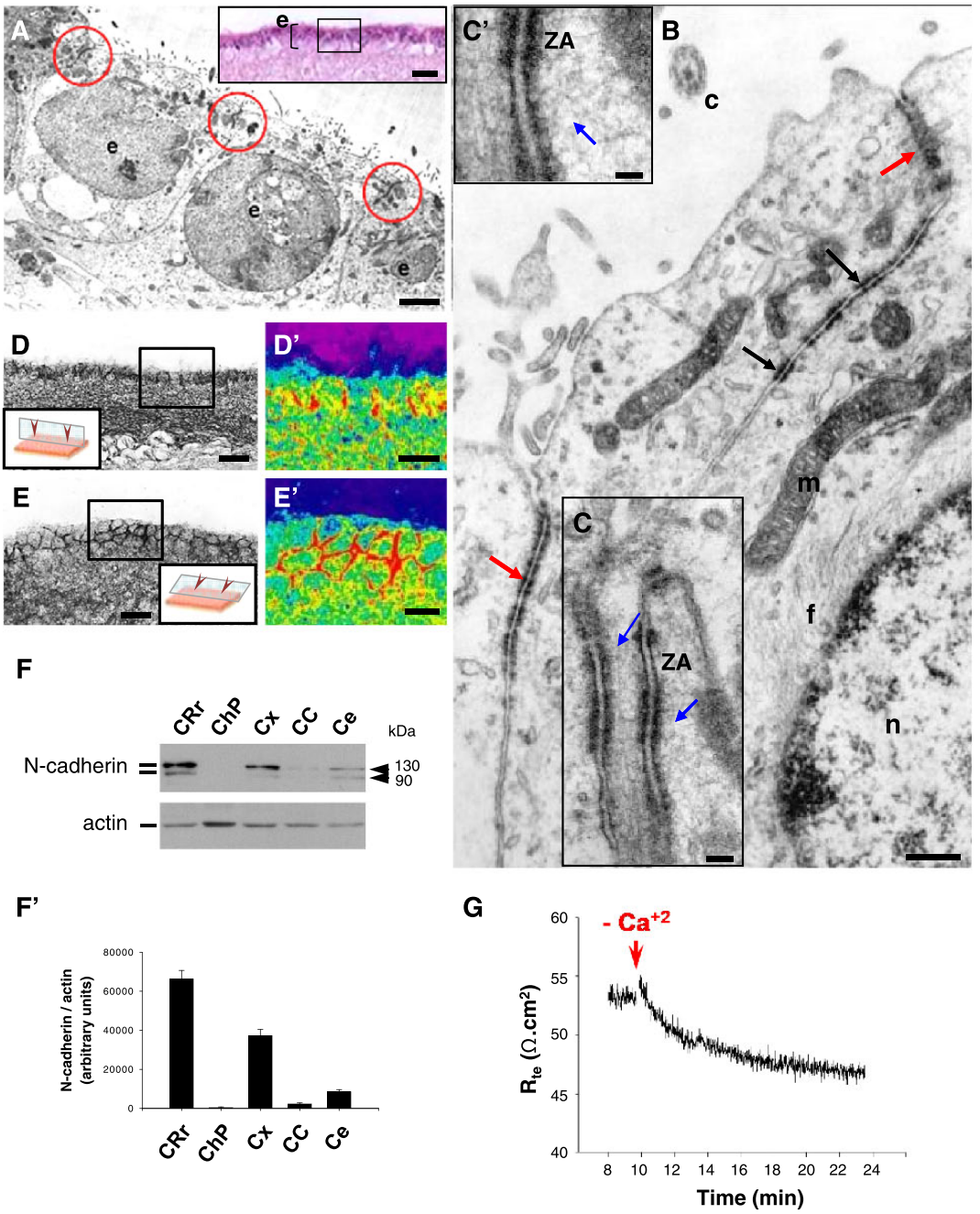

FIGURE 2. Ependymal cells are joined together by N-cadherin–based zonula adherens junctions. **(A)** Transmission electron microscopy (TEM) of a 1-day in vitro (DIV) explant from collicular recess roof (CRr). Red circles highlight adherens junctions between ependymal cells (e). Inset: Reference image of a CRr stained with hematoxylin and eosin (H/E). **(B)** Apical region of 3 neighboring ependymal cells. Adherens junctions are zonula type (red arrows) and macula type (black arrows). n, nucleus; f, bundle of microfilaments; c, cilium; m, mitochondria. **(C)** High-power magnification of adherens junctions (ZA). There is a honeycomb-like network of actin-like microfilaments (blue arrows) associated with the densities located at the plasma membrane **(C′)**. Detailed view of **(C)** showing the network of actin-like filaments (blue arrow) associated with adherens junctions (ZA). **(D–E)** Perpendicular **(D, D′)** and tangential **(E, E′)** of CRr sections immunostained for N-cadherin. Insets: Schematic view of the orientation of the sections. **(D′)** and **(E′)** are magnified and pseudocolored images of the regions shown in **(D)** and **(E)**. Note the linear **(D′)** and honeycomb-like or zonula-type **(E′)** strong immunoreaction (red) in the lateral membranes of ependymal cells. **(F)** Western blot analysis of CRr and different regions (cell types) of adult bovine brain. ChP, choroid plexus; Cx, cerebral cortex; CC, corpus callosum; Ce, cerebellum. **(F′)** Densitometric analysis. Data represent the mean ± SEM of 3 independent experiments. **(G)** Transependymal resistance (R_{te}) in calcium switch experiments. The R_{te} before depletion of extracellular calcium in the ependymal surface ($-Ca^{+2}$) was approximately 55 $\Omega.cm^2$. The plot is representative of 4 independent experiments. Scale bars = **(A)** 2 μm (inset in **[A]**, 20 μm); **(B)** 400 nm; **(C)** 120 nm; **(C′)** 60 nm; **(D, E)** 20 μm; **(D′, E′)** 10 μm.

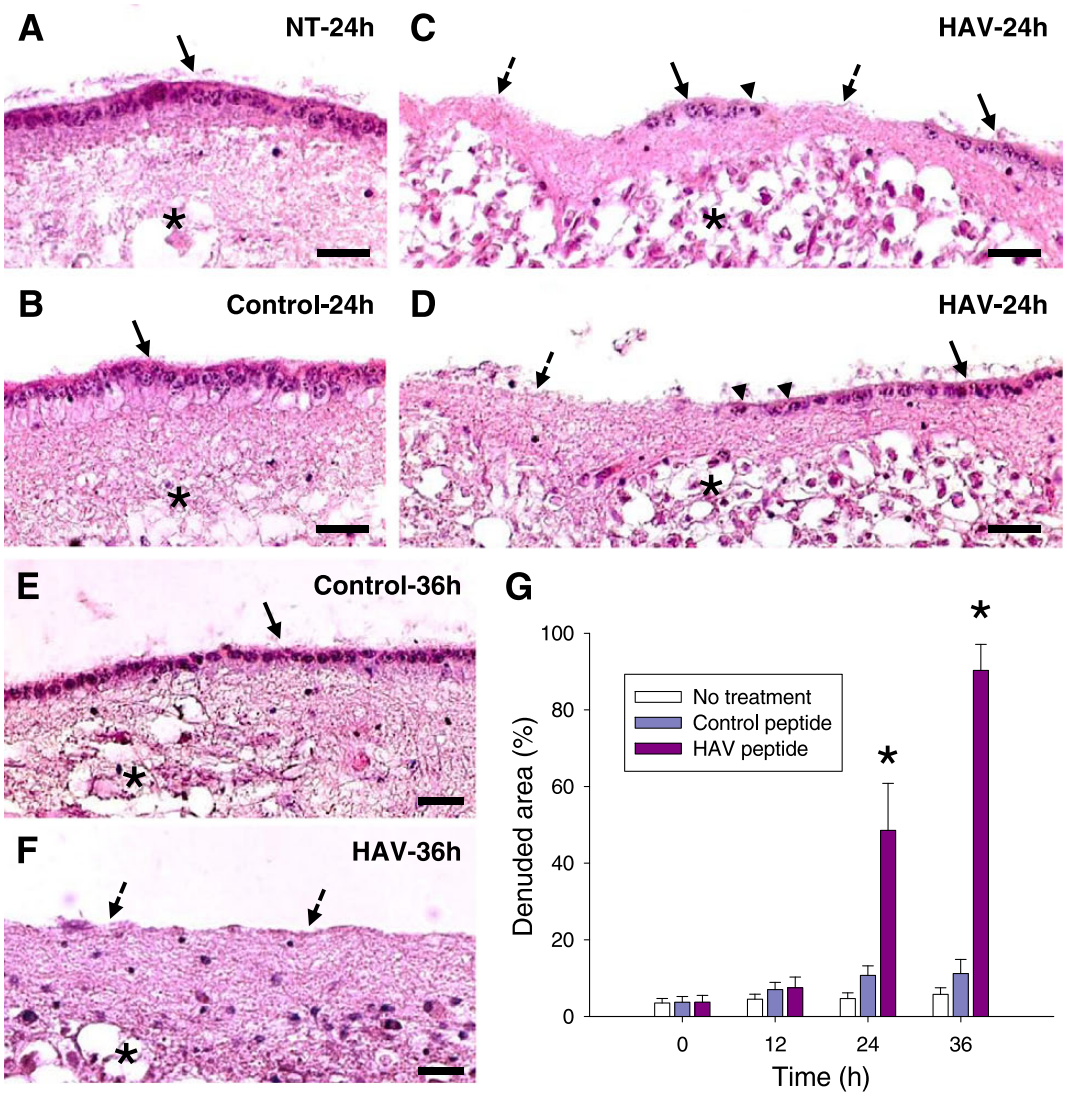

FIGURE 3. Blocking N-cadherin function in explants from bovine collicular recess roof (CRr) leads to ependymal denudation. **(A–F)** Representative images of explants that did not receive treatment for 24 hours **(A)**, explants that were treated with control peptide (400 μg/mL) for 24 hours **(B)** and 36 hours **(E)**, and explants that were treated with N-cadherin–blocking peptide (400 μg/mL) for 24 hours **(C, D)** and 36 hours **(F)**. Blocking peptide contains the homophilic interaction sequence His-Ala-Val (HAV). Denuded areas (dashed arrows) were found together with altered (arrowhead) and apparently normal (full arrows) ependyma. Asterisks: axonal bundles in periaqueductal neural tissue. **(G)** Quantitative analysis of denuded areas in different experimental conditions. Data represent mean (%) ± SEM (n = 10 in each experimental condition). * $p < 0.01$ (ANOVA, Tukey posttest). Scale bar = **(A–F)** 20 μm.

K for 30 minutes at RT. Hybridization with biotinylated nucleotides and recombinant terminal deoxynucleotidyltransferase was done at 37°C for 1 hour according to the manufacturer's guidelines. Sections were then incubated sequentially with streptavidin–horseradish peroxidase (1:500 in PBS for 30 minutes at RT) and 3,3′-diaminobenzidine tetrahydrochloride (10 minutes at RT). Controls included the TUNEL reaction mixture without recombinant terminal deoxynucleotidyltransferase (negative control) and samples treated with 5 to 10 U/mL DNaseI (positive control).

Transmission Electron Microscopy

Collicular recess roof explants were processed for transmission electron microscopy (TEM) as previously described (4). Basically, a triple aldehyde mixture containing 4% paraformaldehyde, 2% glutaraldehyde, and 2% acrolein in 0.2 mol/L phosphate buffer, pH 7.4 was used as fixative (29). Samples were postfixed in 1% OsO_4 in 0.1 mol/L phosphate buffer for 2 hours at 4°C and embedded in Epon. Blocks of tissue were oriented to obtain sections perpendicular to the ependymal surface. Ultrathin sections were contrasted with uranyl acetate and lead citrate and analyzed under a Hitachi H-700 electron microscope.

SDS-PAGE and Immunoblotting

Protein extracts from different regions (cell types) of adult bovine brain were analyzed by Western blotting. The following samples were used: CRr; choroid plexus, brain

cortex; corpus callosum; and cerebellum. Two percent (vol/vol) 2-mercaptoethanol was added to the samples. After boiling for 2 minutes, 15 mg (CRr, brain cortex, corpus callosum, and cerebellum) or 30 mg (choroid plexus) of total protein were loaded on 10% polyacrylamide gels according to Laemmli (30). The proteins were then transferred to polyvinylidene fluoride membranes (Millipore, Bedford, MA). Blots were incubated for 1 to 2 hours at 37°C with anti–N-cadherin antibody (H-63; Santa Cruz Biotechnology) diluted 1:1000 in PBS containing 0.05% Tween-20 and 1% bovine serum albumin. Horseradish peroxidase–conjugated goat anti–mouse IgG was used as secondary antibody (0.25 mg/mL for 30 minutes at 37°C). Excess antibodies were removed by washing 5 × 5 minutes in 1× PBS. Detection was accomplished with an enhanced chemiluminescence system (SuperSignal West Pico Chemiluminescent Substrate, Pierce, Rockford, IL) and subsequent exposure to Kodak XAR film (Eastman Kodak, Rochester, NY) for 5 to 30 seconds. To confirm equal loading of proteins, blots were stripped and reprobed with a mouse monoclonal anti-actin antibody (1:1000; JLA20, Developmental Studies Hybridoma Bank, University of Iowa, Iowa City, IA).

Electrophysiological Studies (Calcium Switch Assays)

Pairs of equal-sized pieces of CRr explants were mounted in tissue-holding sliders (aperture of 0.1 cm^2) and placed as a dividing membrane in a modified Ussing chamber (Physiologic Instruments, San Diego, CA). Both tissue sides were bathed at 37°C in 4 mL of bath solution with calcium (BS + Ca) (120 mmol/L NaCl, 25 mmol/L $NaHCO_3$, 3.3 mmol/L KH_2PO_4, 0.8 mmol/L K_2HPO_4, 1.2 mmol/L $MgCl_2$, 1.2 mmol/L $CaCl_2$) supplemented with 10 mmol/L d-glucose and gassed with 95% O_2 and 5% CO_2. Under these conditions, the tissue was allowed to equilibrate for 10 to 15 minutes before the experiment was started. Because they were performed as paired experiments, one tissue sample served as control and the other as experimental (calcium switch). Calcium switch was achieved by fast replacing BS + Ca solution in the ventricular (ependymal) surface of the tissue sample for BS solution without 1.2 mmol/L $CaCl_2$ and supplemented with 2 mmol/L EGTA, as previously described (31). The short-circuit current (I_{sc}) (an indicator of net ion transport taking place across the tissue) was continuously measured (VCC MC2 amplifier;

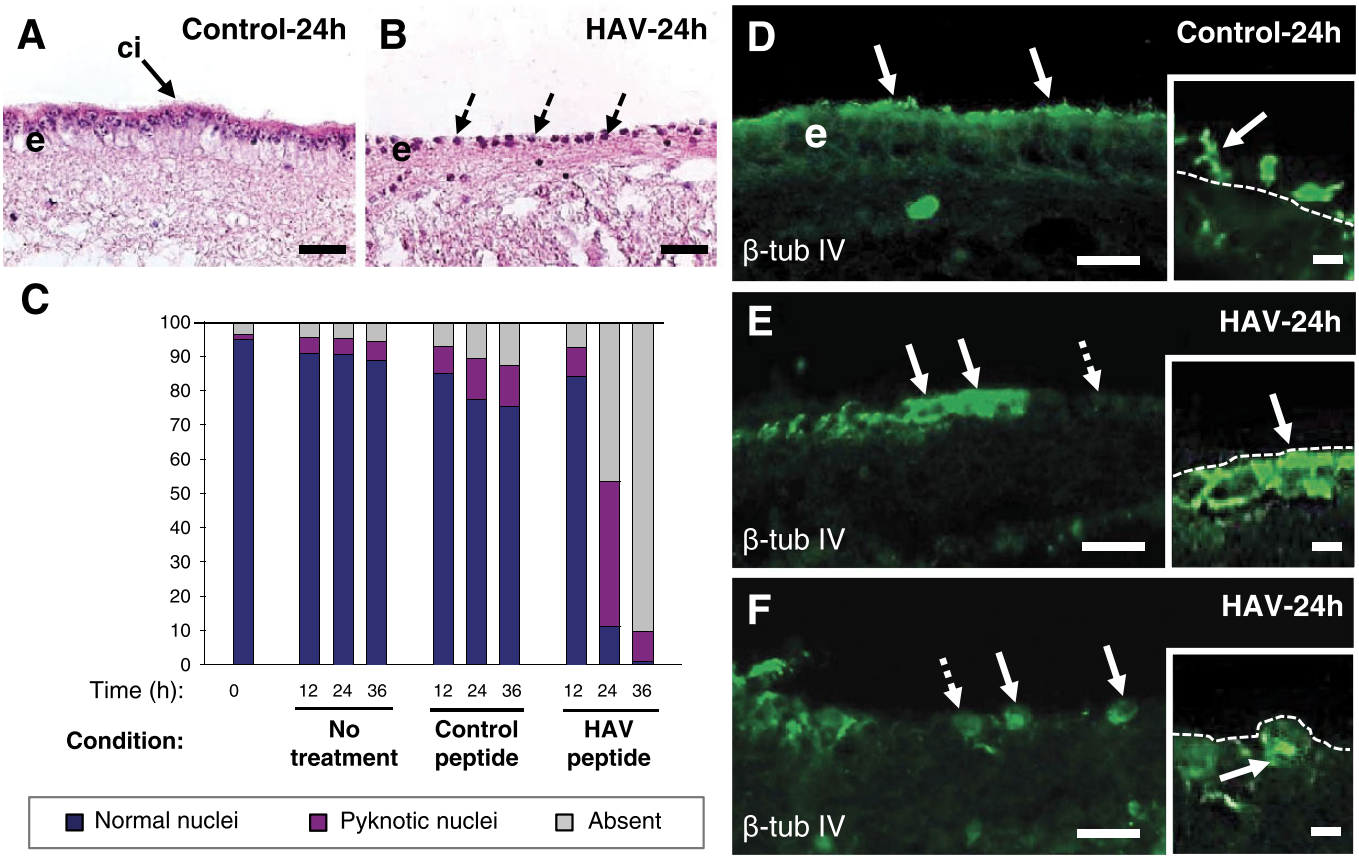

FIGURE 4. Disruption of N-cadherin–based cell-cell adhesion leads to morphological changes in ependymal cells. **(A)** Explant treated with control peptide (400 μg/mL) for 24 hours. Ependymal cells are cubic to columnar and multiciliated (ci). **(B)** In an explant treated with HAV blocking peptide (400 μg/mL) for 24 hours, there are condensed (pyknotic) nuclei (arrowheads) and shrinkage of ependymal cells (dotted arrows). **(C)** Ratios of normal to altered cells per area (%) (n = 10 in each experimental condition). **(D–F)** β-IV tubulin (β-IV tub, cilia marker) immunostaining. **(D)** In controls, β-IV tubulin immunoreaction is polarized in the multiciliated apical region of ependymal cells (arrows). **(E, F)** In explants treated with HAV blocking peptide, β-IV tubulin is less polarized and abnormally distributed (white arrows) or absent (broken arrows). Scale bars = **(A, B, D–F)** 20 μm (insets in **[D–F]** 5 μm).

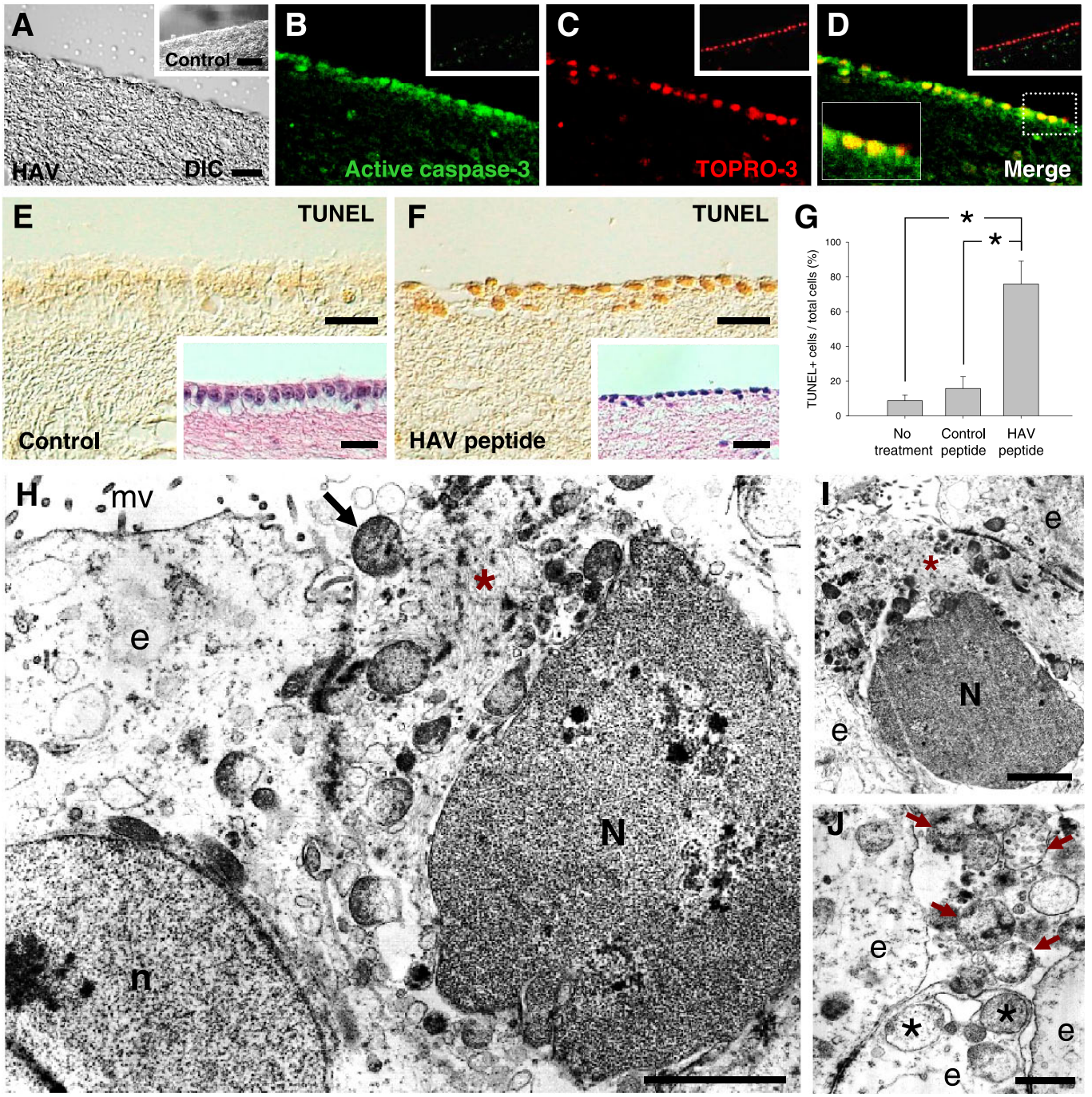

FIGURE 5. Disruption of N-cadherin–based cell-cell adhesion triggers apoptosis of ependymal cells. **(A–D)** Immunofluorescent detection of active caspase-3 in ependymal cells of explants treated with HAV blocking peptide (400 μg/mL) for 24 hours. TOPRO-3 was used for DNA (nuclear) staining. Note that cells with condensed chromatin (pyknotic nuclei) are strongly stained with TOPRO-3 (hyperchromasia) and anti–active caspase-3 (inset in **[D]**). DIC, differential interference contrast microscopy of Nomarski. **(E–G)** TUNEL assay. Representative images of explants treated with control peptide **(E)** or HAV peptide **(F)**. **(G)** Quantification of TUNEL-positive ependymal cells (* $p < 0.01$; ANOVA, Tukey posttest). **(H–J)** Transmission electron microscopy of explants treated with HAV blocking peptide for 24 hours. Many ependymal cells show characteristic apoptotic changes, such as plasmalemmal blebbing (arrow in **[H]**), altered electron density of cytoplasm (red asterisks in **[H]** and **[I]**), and nuclear chromatin condensation [N]. **(H)** Note that the ependymal cell (e) adjacent to the apoptotic cell shows an apparently normal appearance with a normal electron density of cytoplasm, microvilli (mv), and euchromatic nucleus (n), with evident nucleolus. **(J)** Apical region of 3 ependymal cells (e). Note the presence of heterogeneous apoptotic bodies (red arrows) and endosome/phagosome-like structures (asterisks) in the subapical region of the ependymal cells. Scale bars = **(A–F)** 20 μm (insets **[A–D]** 50 μm); **(H–I)** 2 μm; **(J)** 1 μm.

Physiologic Instruments). The voltage was clamped to 0 mV, and 400-millisecond pulses of ±10 mV were passed across the tissues at 1-second intervals using the Acquire & Analyze 2.3 version software and a DI-720 interface (DataQ Instruments, Akron, OH). Transependymal resistance (R_{te}) was calculated from the experimental data using Ohm law. Values of R_{te} were expressed in $\Omega.cm^2$.

Data Analysis

Each N-cadherin function–blocking experiment was repeated at least 10 times, with triplicates of each condition. Image analyses were performed in 5 serial sections per sample using ImageJ software (ImageJ 1.45; NIH, Bethesda, MD). Data were statistically analyzed on commercially available software (Graphpad Prism 4.01; Graphpad Software, Inc., San Diego, CA) by analysis of variance (ANOVA), followed by Tukey posttest for multiple comparisons, with $p < 0.05$ considered significant.

RESULTS

Ependymal Cells Are Joined Together by Functional N-Cadherin–Based Zonula Adherens Junctions

In the bovine brain, the CRr is a thin sheet of neural tissue (Fig. 1A, B). The CRr explants were a flat tissue sheet, approximately 150-μm thick (Fig. 1C), formed by ependyma, a neuropil rich in GFAP-positive astrocytes and axon bundles, and the pial membrane (Fig. 1D, E). After 36 hours in vitro, the explants were viable and showed no structural differences compared with fresh explants, and ependymal cells had vigorous ciliary beating and a strong immunoreaction for functional markers such as caveolin-1 (Fig. 1F).

Ultrastructural analysis showed that ependymal cells were joined together by a set of well-developed zonula- and macula-type adherens junctions (Fig. 2A–C). There was a honeycomb network of actin-like filaments, and some filaments 10 nm in diameter associated with the densities located at the plasma membrane (Fig. 2C, C′). Gap junctions were also identified, but TJs were not seen (Fig. 2B, C). Expression of occludin and claudin-1 in the ependymal lining of CRr explants was undetectable by immunohistochemistry (data not shown). Adherens junctions formed a continuous adhesion belt (or zonula *adherens*) in the most apical region of the lateral domain of the plasma membrane (Fig. 2A–E′). They were not immunoreactive for E-cadherin but were strongly immunoreactive to N-cadherin (Fig. 2D, E′). In tangential sections, N-cadherin immunoreaction showed a distinctive honeycomb-like pattern of zonula-type adherens junctions (Fig. 2E, E′). Immunoblot studies revealed that N-cadherin was highly expressed in CRr explants (enriched in ependymal cells) as compared with other brain regions (Fig. 2F, F′).

Functionality of adherens junctions was confirmed by electrophysiological studies. Because calcium is critical for adherens junctions function, we evaluated transependymal resistance in Ussing chamber experiments under calcium switch conditions. Collicular recess roof explants were dissected, mounted in Ussing chambers, and maintained under voltage clamp. The transependymal resistance values (R_{te} in $\Omega.cm^2$) were calculated over time in the presence (2 mmol/L $CaCl_2$) and absence (0 mmol/L $CaCl_2$ + 2 mmol/L EDTA) of calcium in the ventricular (ependymal) side of the explants, as described in Material and Methods. Interestingly, R_{te} values before calcium depletion were approximately 55 $\Omega.cm^2$, which are compatible with a relative permissive barrier, that is, absence of TJs (Fig. 2G). After calcium depletion, R_{te} values showed a significant decrease (Fig. 2G), suggesting that calcium-dependent adherens junctions play a major role in R_{te} properties in this ependymal preparation.

Blocking N-Cadherin Function Leads to Ependymal Denudation of Ventricular Walls

To test the role of N-cadherin–based adherens junctions in ependymal cytoarchitecture and physiology, we assessed the consequences of N-cadherin functional blockage using an HAV-containing mimetic peptide. The HAV motif is a highly conserved region in the first extracellular domain of all classical cadherins and is thought to be crucial for mediating homophilic cadherin-based intercellular adhesions (32). Treatment with the HAV mimetic peptide for 12 hours showed no difference as compared with controls; however, after 24 hours of treatment, approximately 50% of the ependymal surface of CRr explants was devoid of ependymal cells compared with controls (Fig. 3A–D, G). After 36 hours, HAV peptide provoked massive denudation of more than 90% of the ependymal surface (Fig. 3E–G). Collectively, these findings confirm that intercellular adhesion of ependymal cells is critically dependent on N-cadherin. Furthermore, they show that defects in N-cadherin–based junctions are sufficient to provoke ependymal denudation.

Apoptosis of Ependymal Cells Precedes Ependymal Denudation

To assess the mechanism responsible for ependymal denudation after HAV peptide treatment, we first investigated the cytological and morphological changes in ependymal cells before denudation. After 24 hours of treatment with HAV peptide, approximately 50% of the ependymal surface was denuded and the other approximately 50% remained lined by ependymal cells (Figs. 3G; 4C, blue + purple bars); however, most of these cells showed dramatic morphological apoptotic-like changes (33–35). Indeed, approximately 79% of these ''still'' resistant cells showed condensation of nuclear chromatin, scarce cytoplasm (cell shrinkage) with enlarged intercellular spaces, and reduction or absence of cilia (Fig. 4A–C). The polarized distribution of the cilia marker β-IV tubulin was lost in most altered ependymal cells after HAV peptide treatment (Fig. 4D–F).

To assess whether these changes corresponded to apoptotic changes, explants were immunostained using specific antibodies against the active form of caspase-3, one of the key executors of apoptosis (36, 37) (Fig. 5A–D). Most of the altered ependymal cells were immunoreactive to active caspase-3 (Fig. 5B), and those cells with pyknotic nuclei (i.e. condensed chromatin strongly stained with fluorescent dyes such as TOPRO-3) showed the strongest immunoreaction to active caspase-3 (Fig. 5D inset). These results were confirmed

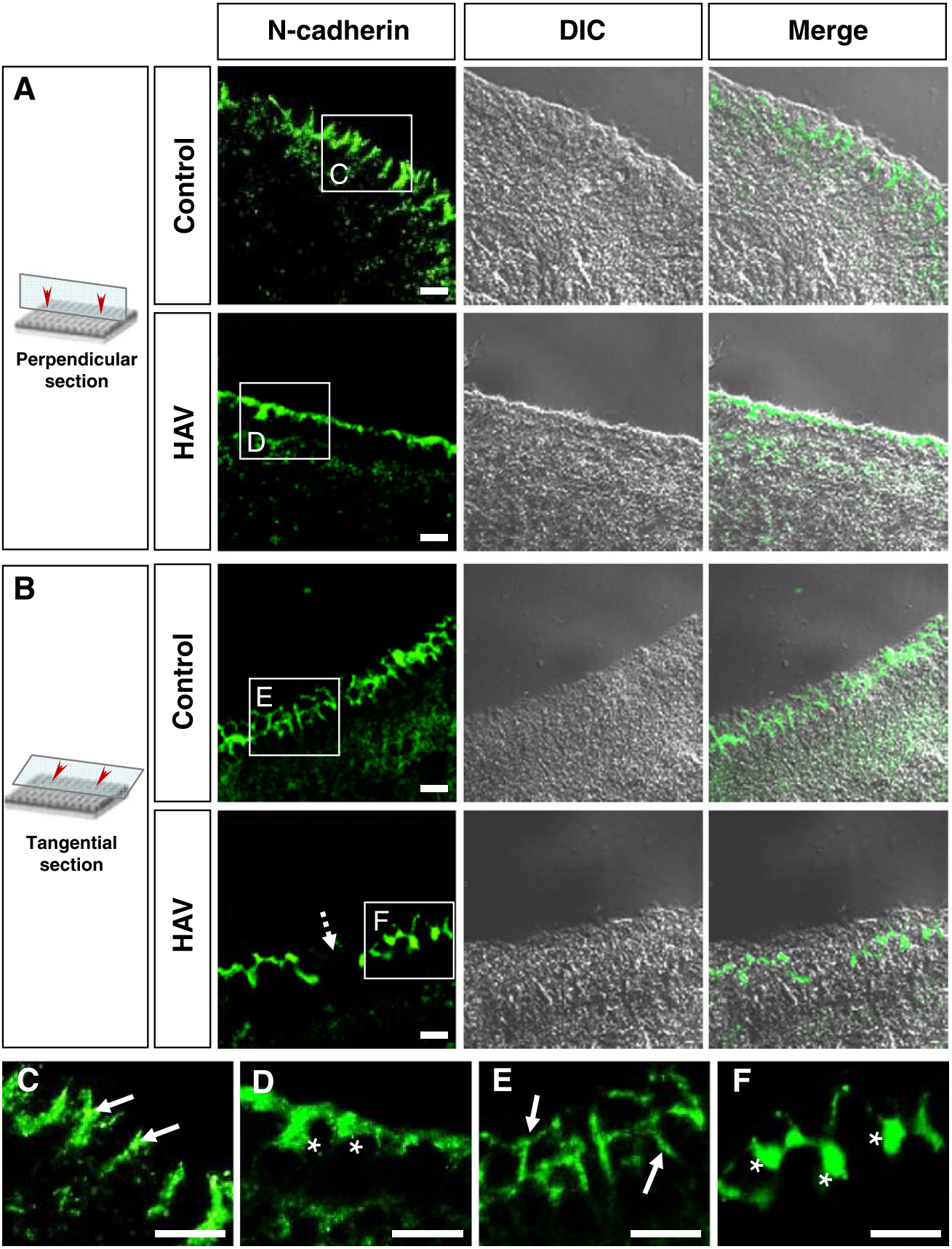

quantitatively by TUNEL assays (Fig. 5E-G). The number of TUNEL-positive cells was increased 5-fold in HAV-treated explants compared with controls (75.9% of ependymal cells were TUNEL positive after HAV peptide treatment vs 15.8% in control peptide treatment after 24 hours) (Fig. 5G). Moreover, HAV-treated explants had several typical ultrastructural changes associated with apoptosis, such as condensation of the cytoplasm and appearance of fibrillar structures (Fig. 5H–I), which are considered signs of cell dehydration, one of the early events of apoptosis (33–35). Pronounced vacuolization of the cytoplasm, disappearance of microvilli, and fragmentation/segregation of nucleolar material, events associated with the initial steps of apoptosis, were also identified (Fig. 5H, I). Condensed and highly uniform nuclear chromatin (Fig. 5H, I) and formation of surface blebs leading to apoptotic bodies (Fig. 5H, J), considered 2 of the most characteristic features of apoptosis (33, 38), were also observed in the explants treated with HAV peptide. Finally, signs of active phagocytosis of apoptotic bodies by adjacent ependymal cells were observed (Fig. 5J). These results indicate that apoptosis of ependymal cells precedes denudation of ventricular walls after N-cadherin function–blocking treatment.

Early Changes Caused by N-Cadherin Blockage in Ependymal Cells

Previous studies have indicated that the disruption of the homophilic interaction between cadherins leads to alterations in the dynamics of trafficking/recycling of these proteins, favoring their endocytosis (39, 40); this, in turn, provokes defects in adherens junctions stability and function. Although N-cadherin blockage resulted in massive apoptotic changes in most ependymal cells after 24 hours, approximately 21% of ependymal cells showed normal appearances at this time point (Fig. 4C, blue bar). These cells were excellent materials to study early changes provoked by N-cadherin blockage preceding or triggering the onset of apoptosis and ependymal denudation. Thus, we selected regions with abundant normal-appearing ependymal cells and analyzed them by immunofluorescence and confocal microscopy and TEM.

Perpendicular and tangential serial sections from CRr explants were immunostained for N-cadherin to study the subcellular distribution of N-cadherin after HAV peptide treatment. In control explants, most of the ependymal cells showed the typical immunostaining patterns characterized by a linear (perpendicular sections, Fig. 6A, C) or honeycomb-like (tangential sections, Fig. 6B, E) immunoreaction in the lateral plasma membrane. By contrast, in explants treated with HAV peptide, these patterns were virtually absent, and abnormal intracellular accumulations of N-cadherin–immunoreactive material were observed in the subapical region of ependymal cells (Fig. 6A, B, D, F). Transmission electron microscopy showed that ependymal cells of CRr explants treated with HAV peptide had a dramatic reduction in the extension of the electron densities of adherens junctions and, in some cases, these densities were asymmetrically distributed (Fig. 7A–E). Widening of the intercellular space between ependymal cells was also observed (Fig. 7F).

DISCUSSION

A Novel Organotypic Culture System to Study Ependymal Physiology and Pathophysiology

There are few culture systems designed to study ependymal architecture, physiology, and pathophysiology. Primary and monolayer cultures have been used (41). However, these types of cultures are not suitable to investigate various in vivo–like conditions because they lack some types of cell-to-cell interactions. These interactions are known to influence gene expression and, consequently, the architecture and physiology of cells. Indeed, under primary culture conditions, ependymal cells show morphological and immunocytochemical differences from ependymal cells in vivo (41). Perez-Martin et al (42) have developed an organotypic culture system of ependymal explants obtained by gently scraping the surface of the adult bovine lateral ventricles. Although this system seems to reproduce in vivo cellular relationships better than monolayer cell cultures, several phenotypic changes in ependymal cells of such explants have also been described. We have developed and characterized a novel organotypic culture system to study ependymal physiology and pathophysiology. Explants from bovine CRr prepared and cultured as described here mimic in vivo tissue architecture and incorporate aspects of cell-cell interactions that cannot be evaluated in other culture conditions. Furthermore, our model can be used to study not only the cellular and molecular mechanisms of ependymal disruption but also the response of the subependymal tissue to such a disruption. It has been recently described that ependymal denudation of brain ventricular walls in hydrocephalic mutant mice and humans triggers a reaction of subependymal astrocytes that covers denuded walls and acquire some ependymal-like features (43). This phenomenon and the mechanisms involved in such a reaction could be further investigated in the model described here.

Ependymal Cells Are Joined Together by N-Cadherin–Based Adherens Junctions

Most epithelial cells forming a simple epithelium are joined together by junctional complexes including TJs, whereas

FIGURE 6. Disruption of N-cadherin–based adhesion provokes changes in N-cadherin subcellular distribution. **(A, B)** Perpendicular **(A)** and tangential **(B)** sections of the ventricular wall of the bovine collicular recess roof (CRr) immunostained for N-cadherin. Schematic views of the orientation of the sections are shown. Representative images from control and HAV peptide–treated explants are shown. Note the abnormal subcellular distribution of N-cadherin immunoreaction in HAV peptide–treated explants. In tangential sections **(B)**, there is lack of continuity in the honeycomb-like pattern (dotted arrow in **[B]**). Squares correspond to the regions shown in **(C–F)**. DIC, differential interference contrast microscopy of Nomarski. **(C–F)** High magnification of the regions depicted in **(A)** and **(B)**. Blocking N-cadherin function provokes intracellular accumulation of N-cadherin immunoreactive material (asterisks in **[D]** and **[F]**) and reduction of the normal linear or honeycomb-like N-cadherin pattern (arrows in **[C]** and **[E]**). Scale bar = **(A–F)** 20 μm.

multiciliated ependymal cells do not display TJs (8, 18, 19). Functional and immunohistochemical studies have demonstrated that continuous TJs between neuroepithelial cells virtually disappear during neural tube closure in early stages of brain development (WS 8–9 in mouse) (44), and only low or undetectable expression of TJs proteins persists in the

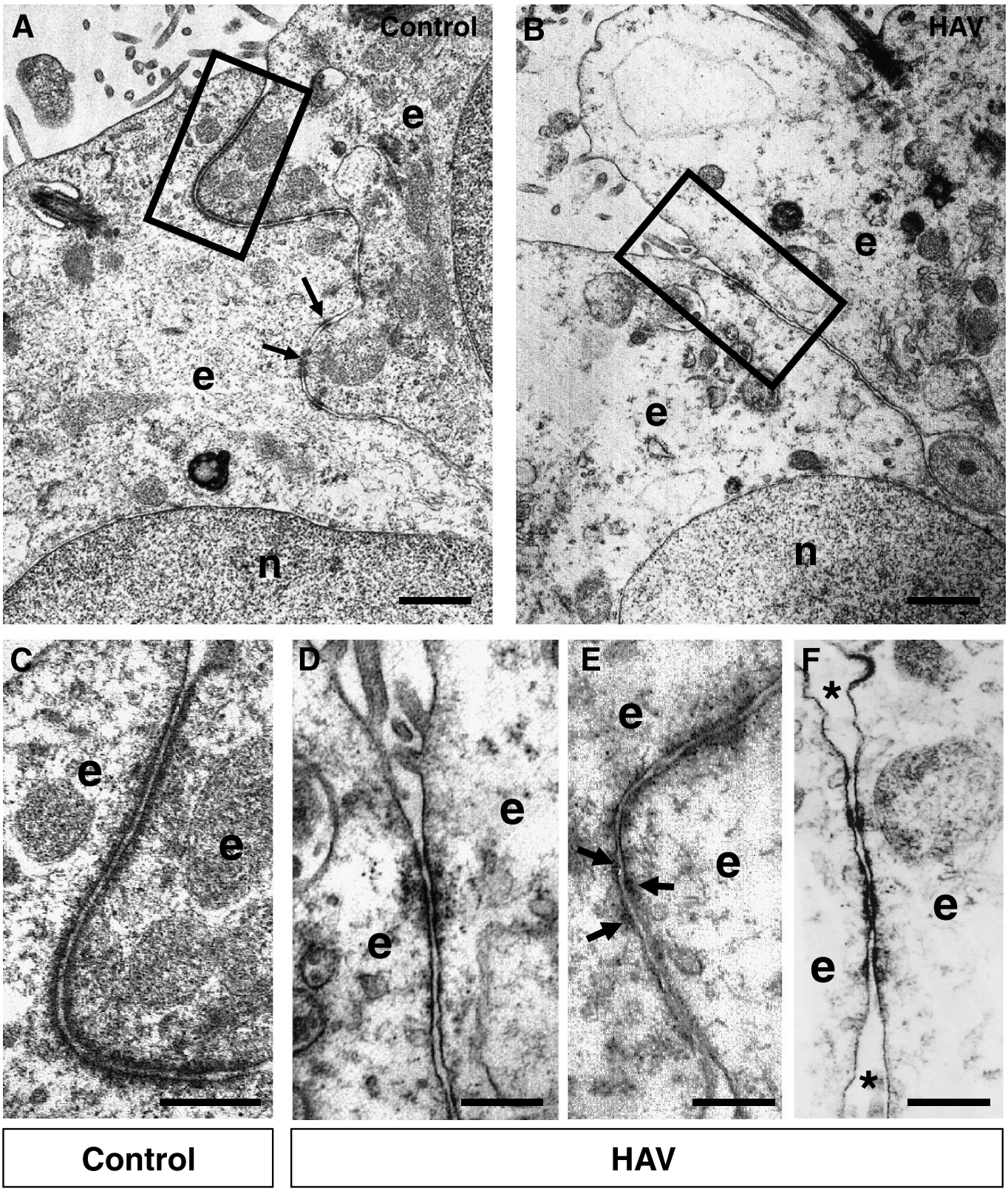

mature multiciliated ependyma (45). In agreement with these data, our ultrastructural and immunohistochemical results indicate that adult bovine ependymal cells are devoid of TJs. Furthermore, the low basal values of transependymal resistance in electrophysiological studies are not compatible with the presence of TJs. On the other hand, our data show that adult bovine ependymal cells exhibit well-developed N-cadherin–based adherens junctions at the apical-lateral interface. Likewise, other reports indicate that ependymal cells from human and various animal models are joined together by zonula adherens–type junctions (2, 19, 45, 46).

N-cadherin belongs to the cadherin superfamily of transmembrane glycoprotein adhesion molecules that allow calcium-dependent anchorage of homotypic cell types. N-cadherin has been previously identified as a key component of the adherens junctions localized in the apical end of neuroepithelial/radial glial cells of mouse (47, 48) and chicken (49). More recently, we demonstrated that N-cadherin is highly expressed in mature multiciliated ependymal cells in humans (16). Thus, N-cadherin seems to be one of the main apical junction proteins maintaining the structure and organization of the cells lining the brain ventricular walls from neuroepithelial/radial glial cells to mature ependymal cells in several species.

Disruption of N-Cadherin–Based Cell-Cell Junctions Leads to Sequential Pathological Changes That Precede Ependymal Denudation

Our results demonstrate for the first time that a selective blockage of N-cadherin function in mature ependymal cells is sufficient to provoke ependymal denudation. We summarize the suggested sequence of pathological changes that lead to ependymal denudation after selectively blocking N-cadherin function in Figure 8A. Interfering with N-cadherin homophilic interactions (Fig. 8Aa, b) leads to ultrastructurally abnormal adherens junctions and intracellular accumulation of N-cadherin (Fig. 8Ac). These phenomena suggest that the extracellular blockage of N-cadherin function alters its traffic dynamics. Certainly, the cycling of cadherins represents a cellular process that can impinge on the stability of the adherens junctions (52). Although such cycling is minimal in epithelial monolayers, it is markedly enhanced as cells disassemble their intercellular contacts (39). Our working model of N-cadherin turnover and the consequences of blocking its function by HAV peptides is shown in Figure 8B, C. In this model, loss of cell-cell contacts between ependymal cells (by treatment with HAV mimetic peptide) is accompanied by a concomitant increase in N-cadherin internalization. Correspondingly, Le et al (39) demonstrated in MDCK cells that extracellular calcium depletion disrupts cell-cell contacts and provokes an increase in E-cadherin endocytosis. On the other hand, Ivanov et al (40) observed that after calcium depletion in T84 cell cultures, disruption of adherens junctions was associated with the internalization of cadherins in a subapical cytosolic compartment. Similarly, we also observed accumulation of N-cadherin in a subapical compartment of ependymal cells after HAV peptide treatment. At present, little is known about the molecular regulation of N-cadherin endocytosis/trafficking and the identity of the intracellular compartments involved.

Under our experimental conditions, loss of N-cadherin–based contacts leads to apoptosis of ependymal cells (Fig. 8Ad), which, in turn, seemed to be the mechanism leading to ependymal denudation of ventricular walls in CRr explants (Figs. 8Ae, f). In this context, recent findings indicate that surface adhesion molecules not only serve to keep cells joined together or bound to the extracellular matrix but also behave as receptors initiating intracellular signaling pathways that modulate key cellular events, including survival and proliferation (53). Indeed, the role of cell anchorage for cell survival is now widely accepted, and several reports indicate that different normal (noncancer) cell types undergo apoptosis on loss of cell-cell and/or cell–extracellular matrix attachment (54–56). This type of cell death has been named ''anoikis'' (Greek: state of homelessness) (54–57). Our results suggest that N-cadherin is a key molecule in the complex network of survival signaling in ependymal cells. In line with this idea, N-cadherin–mediated cell contact inhibits apoptosis of granulosa cells during development of ovarian follicles (58, 59). Furthermore, disruption of cadherin-based cell-cell contacts leads to increased apoptosis of primary renal tubular cells (60), cultured endothelial cells (26), and intestinal epithelial cells (61, 62). In addition, studies from Galaz et al (63) have revealed that loss of cadherin-mediated cell-cell adhesion triggers apoptosis in murine keratinocytes under photodynamic treatment. Although signaling pathways of cell-cell adhesion–mediated survival are still poorly understood (55), it has been proposed that cadherin-mediated junctions promote survival in a PI3K/Akt-dependent fashion (60, 61). Cadherins may also regulate cell survival through β-catenin signaling (61, 64) and through a crosstalk with integrin- and receptor tyrosine kinase–dependent signaling pathways (26, 65).

N-Cadherin Disruption and Neuropathology

In humans and rodents, neuroepithelial/ependymal disruption or denudation has been associated with the onset and early stages of different CNS disorders, such as hydrocephalus (4, 15), periventricular heterotopia (17), and SBA (16). In the case of hydrocephalus, there are several animal models in which ependymal denudation is associated with loss-of-function mutations in different genes involved in the formation and maintenance of adherens junctions between the

FIGURE 7. Blocking N-cadherin function leads to ultrastructural modifications in adherens junctions. **(A)** In explants that received no treatment (control), ependymal cells are joined together by large apical zonula adherens–type junctions with symmetric electron densities. Note the presence of macula-type adherens junctions (arrows). Rectangle corresponds to the region shown in **(C)**. **(B)** Explants treated with HAV blocking peptide (400 μg/mL) for 24 hours. There is a dramatic reduction in the extension of zonula adherens junctions and their associated electron densities. Rectangle corresponds to the region shown in **(D)**. **(C)** Detail of adherens junctions between ependymal cells in a control preparation. **(D–F)** Details of various ultrastructural changes in HAV peptide–treated explants. Electron density associated with adherens junctions is severely reduced **(D)** or distributed asymmetrically (arrows in **[E]**). Intercellular spaces seem dilated (asterisk in **[F]**). e, ependymal cells. Scale bars = **(A, B)** 1 μm; **(C–F)** 0.5 μm.

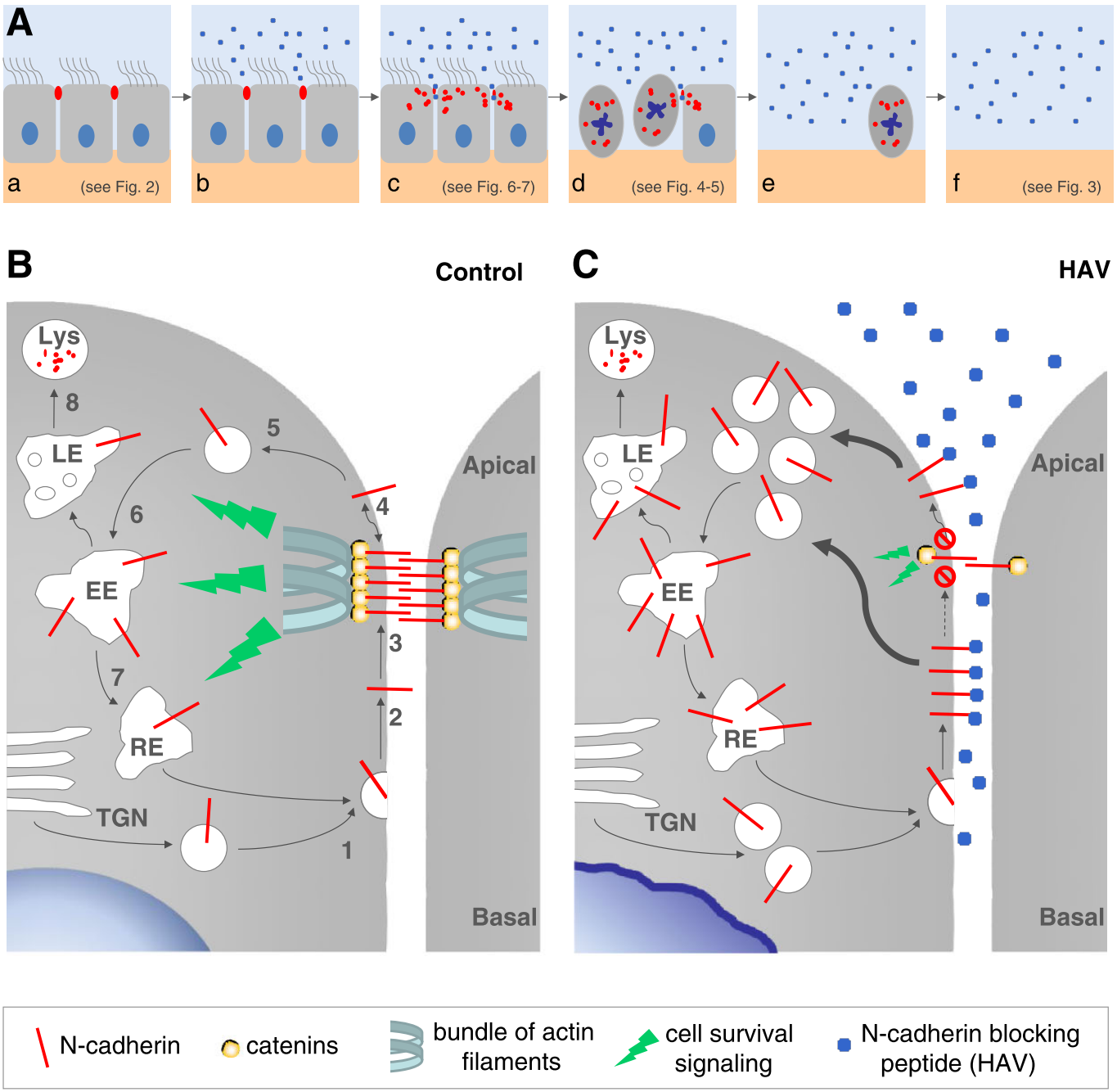

FIGURE 8. Model of N-cadherin trafficking/cycling in ependymal cells and consequences of the treatment with blocking peptides. **(A)** Sequence of events triggered by N-cadherin–blocking peptide (HAV peptide) treatment of ependymal cells. Incubation of collicular recent roof (CRr) explants with HAV peptide **(A, B)** provokes a disruption of N-cadherin–based adherens junctions and an abnormal subcellular distribution of N-cadherin in ependymal cells **(C)**. This, in turn, leads to a regional to massive apoptosis of ependymal cells (d, e) and denudation of CRr walls **(E, F)**. **(B)** Newly synthesized N-cadherin is trafficked from the trans-Golgi network (TGN) to the cell surface [1] (50). Once in the plasma membrane, N-cadherin molecules move laterally within the membrane [2] for incorporation, together with catenins, into adherens-junction complexes [3] (51). Surface N-cadherin is in a dynamic equilibrium between ''free'' and junction-associated molecules [4]. Surface N-cadherin can be endocytosed [5], recycled back to the cell surface [6, 7], or targeted for degradation [8] (39). Interestingly, junction-associated molecules remain stabilized at cell surface and trigger cell survival signals (green rays). **(C)** HAV-blocking peptide inhibits N-cadherin homophilic interactions, disrupts adherens junction complexes, and modifies trafficking dynamics, leading to an accumulation of N-cadherin in intracellular compartments and a reduction in cell survival signaling. EE, early endosomes; RE, recycling endosomes; LE, late endosomes; Lys, lysosomes.

cells forming the ventricular zone from neuroepithelium to ependyma (20, 21, 66–70). Blocking N-cadherin function in the brain of chick embryos using antibodies directed against the extracellular domain of N-cadherin provokes disruption of the neuroepithelial lining (49). Similarly, we recently described that an abnormal subcellular distribution of N-cadherin (and abnormal adherens junctions) likely precedes ependymal denudation in the cerebral aqueduct of human SBA fetuses (16). Thus, N-cadherin–based adherens junctions seem to play a key role not only in mature ependymal cell survival and function but also in the physiology of neuroepithelial, radial glial, and fetal ependymal cells that line ventricular walls during normal and pathologic brain development (70). This is relevant not only because these cells are histologically distinct from mature ependymal cells (2, 71, 72) but also because neuroepithelial and radial glial cells are the neural stem cells during the embryonic neuro/gliogenic period (71). In this context, defects in adherens junctions during early embryonic brain development, particularly in relation to genetically programmed disorders, may interfere with the fate of neural stem cells, including the initial differentiation of neurons, astrocytes, and fetal ependymal cells. On the other hand, disruption of cell-cell junctions in late embryonic or postnatal stages would trigger ependymal apoptosis and denudation. In this context, Yung et al (73) have recently reported that lysophosphatidic acid signaling can trigger posthemorrhagic hydrocephalus by disrupting N-cadherin–based adherens junctions in the neuroependymal lining.

In summary, our results show that 1) organotypic culture of CRr explants is a useful ex vivo model for investigating ependymal architecture, physiology, and pathophysiology; 2) N-cadherin plays a key role in ependymal cytoarchitecture and function; 3) ependymal cells seem to be protected from apoptosis through the establishment/maintenance of N-cadherin–based cell-cell contacts; and 4) disruption of N-cadherin–based adherens junctions is sufficient to trigger ependymal denudation. Thus, we propose that a defect in N-cadherin–based junctions is a pathogenic common pathway to different inherited or acquired CNS disorders associated with ependymal denudation.

ACKNOWLEDGMENTS

The authors thank Dr. Conrad Johanson for critical reading of the manuscript and acknowledge the technical support of Mr. Claudio Lizama for processing TEM preparations. Monoclonal antibodies against actin (JLA20), developed by Jim Jung-Ching Lin, were obtained from the Developmental Studies Hybridoma Bank (DSHB) developed under the auspices of the NICHD and maintained by The University of Iowa, Department of Biological Sciences, Iowa City, Iowa.

REFERENCES

1. Bruni JE, Del Bigio MR, Clattenburg RE. Ependyma: Normal and pathological. A review of the literature. Brain Res 1985;356:1–19
2. Del Bigio MR. Ependymal cells: Biology and pathology. Acta Neuropathol 2010;119:55–73
3. Rodriguez EM, Blazquez JL, Guerra M. The design of barriers in the hypothalamus allows the median eminence and the arcuate nucleus to enjoy private milieus: The former opens to the portal blood and the latter to the cerebrospinal fluid. Peptides 2010;31:757–76
4. Wagner C, Batiz LF, Rodriguez S, et al. Cellular mechanisms involved in the stenosis and obliteration of the cerebral aqueduct of hyh mutant mice developing congenital hydrocephalus. J Neuropathol Exp Neurol 2003; 62:1019–40
5. Spassky N, Merkle FT, Flames N, et al. Adult ependymal cells are postmitotic and are derived from radial glial cells during embryogenesis. J Neurosci 2005;25:10–18
6. Batiz LF, Jimenez AJ, Guerra M, et al. New ependymal cells are born postnatally in two discrete regions of the mouse brain and support ventricular enlargement in hydrocephalus. Acta Neuropathol 2011;121:721–35
7. Sarnat HB. Role of human fetal ependyma. Pediatr Neurol 1992;8: 163–78
8. Del Bigio MR. The ependyma: A protective barrier between brain and cerebrospinal fluid. Glia 1995;14:1–13
9. Ibanez-Tallon I, Pagenstecher A, Fliegauf M, et al. Dysfunction of axonemal dynein heavy chain Mdnah5 inhibits ependymal flow and reveals a novel mechanism for hydrocephalus formation. Hum Mol Genet 2004; 13:2133–41
10. Nelson DJ, Wright EM. The distribution, activity, and function of the cilia in the frog brain. J Physiol 1974;243:63–78
11. Town T, Breunig JJ, Sarkisian MR, et al. The stumpy gene is required for mammalian ciliogenesis. Proc Natl Acad Sci U S A 2008;105:2853–58
12. Lechtreck KF, Delmotte P, Robinson ML, et al. Mutations in Hydin impair ciliary motility in mice. J Cell Biol 2008;180:633–43
13. Banizs B, Pike MM, Millican CL, et al. Dysfunctional cilia lead to altered ependyma and choroid plexus function, and result in the formation of hydrocephalus. Development 2005;132:5329–39
14. Jimenez AJ, Tome M, Paez P, et al. A programmed ependymal denudation precedes congenital hydrocephalus in the hyh mutant mouse. J Neuropathol Exp Neurol 2001;60:1105–19
15. Dominguez-Pinos MD, Paez P, Jimenez AJ, et al. Ependymal denudation and alterations of the subventricular zone occur in human fetuses with a moderate communicating hydrocephalus. J Neuropathol Exp Neurol 2005;64:595–604
16. Sival DA, Guerra M, den Dunnen WF, et al. Neuroependymal denudation is in progress in full-term human foetal spina bifida aperta. Brain Pathol 2011;21:163–79
17. Ferland RJ, Batiz LF, Neal J, et al. Disruption of neural progenitors along the ventricular and subventricular zones in periventricular heterotopia. Hum Mol Genet 2009;18:497–516
18. Rodriguez P, Bouchaud C. The supra-ependymal innervation is not responsible for the repression of tight junctions in the rat cerebral ependyma. Neurobiology (Bp) 1996;4:185–201
19. Brightman MW, Reese TS. Junctions between intimately apposed cell membranes in the vertebrate brain. J Cell Biol 1969;40:648–77
20. Imai F, Hirai S, Akimoto K, et al. Inactivation of aPKClambda results in the loss of adherens junctions in neuroepithelial cells without affecting neurogenesis in mouse neocortex. Development 2006;133:1735–44
21. Ma X, Bao J, Adelstein RS. Loss of cell adhesion causes hydrocephalus in nonmuscle myosin II-B–ablated and mutated mice. Mol Biol Cell 2007;18:2305–12
22. Redies C. Cadherins in the central nervous system. Prog Neurobiol 2000; 61:611–48
23. Yap AS, Brieher WM, Gumbiner BM. Molecular and functional analysis of cadherin-based adherens junctions. Annu Rev Cell Dev Biol 1997; 13:119–46
24. Poskanzer K, Needleman LA, Bozdagi O, et al. N-cadherin regulates ingrowth and laminar targeting of thalamocortical axons. J Neurosci 2003;23:2294–305
25. Li G, Satyamoorthy K, Herlyn M. N-cadherin–mediated intercellular interactions promote survival and migration of melanoma cells. Cancer Res 2001;61:3819–25
26. Erez N, Zamir E, Gour BJ, et al. Induction of apoptosis in cultured endothelial cells by a cadherin antagonist peptide: Involvement of fibroblast growth factor receptor-mediated signalling. Exp Cell Res 2004;294: 366–78
27. Noe V, Willems J, Vandekerckhove J, et al. Inhibition of adhesion and induction of epithelial cell invasion by HAV-containing E-cadherin–specific peptides. J Cell Sci 1999;112:127–35

28. Williams E, Williams G, Gour BJ, et al. A novel family of cyclic peptide antagonists suggests that N-cadherin specificity is determined by amino acids that flank the HAV motif. J Biol Chem 2000;275:4007–12
29. Rodriguez EM. Fixation of the central nervous system by perfusion of the cerebral ventricles with a threefold aldehyde mixture. Brain Res 1969; 15:395–412
30. Laemmli UK. Cleavage of structural proteins during the assembly of the head of bacteriophage T4. Nature 1970;227:680–85
31. Flores CA, Cid LP, Sepulveda FV. Strain-dependent differences in electrogenic secretion of electrolytes across mouse colon epithelium. Exp Physiol 2010;95:686–98
32. Shapiro L, Kwong PD, Fannon AM, et al. Considerations on the folding topology and evolutionary origin of cadherin domains. Proc Natl Acad Sci U S A 1995;92:6793–97
33. Hacker G. The morphology of apoptosis. Cell Tissue Res 2000;301:5–17
34. Kerr JF, Wyllie AH, Currie AR. Apoptosis: A basic biological phenomenon with wide-ranging implications in tissue kinetics. Br J Cancer 1972;26:239–57
35. Saraste A. Morphologic criteria and detection of apoptosis. Herz 1999; 24:189–95
36. Springer JE, Nottingham SA, McEwen ML, et al. Caspase-3 apoptotic signaling following injury to the central nervous system. Clin Chem Lab Med 2001;39:299–307
37. Kumar S. Caspase function in programmed cell death. Cell Death Differ 2007;14:32–43
38. Allen RT, Hunter WJ, 3rd, Agrawal DK. Morphological and biochemical characterization and analysis of apoptosis. J Pharmacol Toxicol Methods 1997;37:215–28
39. Le TL, Yap AS, Stow JL. Recycling of E-cadherin: A potential mechanism for regulating cadherin dynamics. J Cell Biol 1999;146:219–32
40. Ivanov AI, Nusrat A, Parkos CA. The epithelium in inflammatory bowel disease: Potential role of endocytosis of junctional proteins in barrier disruption. Novartis Found Symp 2004;263:115–24
41. Prothmann C, Wellard J, Berger J, et al. Primary cultures as a model for studying ependymal functions: Glycogen metabolism in ependymal cells. Brain Res 2001;920:74–83
42. Perez-Martin M, Grondona JM, Cifuentes M, et al. Ependymal explants from the lateral ventricle of the adult bovine brain: A model system for morphological and functional studies of the ependyma. Cell Tissue Res 2000;300:11–19
43. Roales-Bujan R, Paez P, Guerra M, et al. Astrocytes acquire morphological and functional characteristics of ependymal cells following disruption of ependyma in hydrocephalus. Acta Neuropathol 2012;124: 531–46
44. Aaku-Saraste E, Hellwig A, Huttner WB. Loss of occludin and functional tight junctions, but not ZO-1, during neural tube closure: Remodeling of the neuroepithelium prior to neurogenesis. Dev Biol 1996;180: 664–79
45. Alvarez JI, Teale JM. Differential changes in junctional complex proteins suggest the ependymal lining as the main source of leukocyte infiltration into ventricles in murine neurocysticercosis. J Neuroimmunol 2007; 187:102–13
46. Lippoldt A, Jansson A, Kniesel U, et al. Phorbol ester induced changes in tight and adherens junctions in the choroid plexus epithelium and in the ependyma. Brain Res 2000;854:197–206
47. Chenn A, Zhang YA, Chang BT, . Intrinsic polarity of mammalian neuroepithelial cells. Mol Cell Neurosci 1998;11:183–93
48. Kadowaki M, Nakamura S, Machon O, et al. N-cadherin mediates cortical organization in the mouse brain. Dev Biol 2007;304:22–33
49. Ganzler-Odenthal SI, Redies C. Blocking N-cadherin function disrupts the epithelial structure of differentiating neural tissue in the embryonic chicken brain. J Neurosci 1998;18:5415–25
50. Chen YT, Stewart DB, Nelson WJ. Coupling assembly of the E-cadherin/beta-catenin complex to efficient endoplasmic reticulum exit and basal-lateral membrane targeting of E-cadherin in polarized MDCK cells. J Cell Biol 1999;144:687–99
51. Rajasekaran AK, Hojo M, Huima T, et al. Catenins and zonula occludens-1 form a complex during early stages in the assembly of tight junctions. J Cell Biol 1996;132:451–63
52. Palacios F, Tushir JS, Fujita Y, et al. Lysosomal targeting of E-cadherin: A unique mechanism for the down-regulation of cell-cell adhesion during epithelial to mesenchymal transitions. Mol Cell Biol 2005;25:389–402
53. Aplin AE, Howe A, Alahari SK, et al. Signal transduction and signal modulation by cell adhesion receptors: The role of integrins, cadherins, immunoglobulin-cell adhesion molecules, and selectins. Pharmacol Rev 1998;50:197–263
54. Grossmann J. Molecular mechanisms of ''detachment-induced apoptosis—Anoikis.'' Apoptosis 2002;7:247–60
55. Chiarugi P, Giannoni E. Anoikis: A necessary death program for anchorage-dependent cells. Biochem Pharmacol 2008;76:1352–64
56. Taddei ML, Giannoni E, Fiaschi T, et al. Anoikis: An emerging hallmark in health and diseases. J Pathol 2012;226:380–93
57. Frisch SM, Francis H. Disruption of epithelial cell-matrix interactions induces apoptosis. J Cell Biol 1994;124:619–26
58. Peluso JJ, Pappalardo A, Trolice MP. N-cadherin-mediated cell contact inhibits granulosa cell apoptosis in a progesterone-independent manner. Endocrinology 1996;137:1196–203
59. Makrigiannakis A, Coukos G, Christofidou-Solomidou M, et al. N-cadherin–mediated human granulosa cell adhesion prevents apoptosis: A role in follicular atresia and luteolysis? Am J Pathol 1999;154: 1391–406
60. Bergin E, Levine JS, Koh JS, et al. Mouse proximal tubular cell-cell adhesion inhibits apoptosis by a cadherin-dependent mechanism. Am J Physiol Renal Physiol 2000;278:F758–68
61. Hofmann C, Obermeier F, Artinger M, et al. Cell-cell contacts prevent anoikis in primary human colonic epithelial cells. Gastroenterology 2007; 132:587–600
62. Hermiston ML, Gordon JI. In vivo analysis of cadherin function in the mouse intestinal epithelium: Essential roles in adhesion, maintenance of differentiation, and regulation of programmed cell death. J Cell Biol 1995;129:489–506
63. Galaz S, Espada J, Stockert JC, et al. Loss of E-cadherin mediated cell-cell adhesion as an early trigger of apoptosis induced by photodynamic treatment. J Cell Physiol 2005;205:86–96
64. Peluso JJ, Pappalardo A, Hess SA. Effect of disrupting cell contact on the nuclear accumulation of beta-catenin and subsequent apoptosis of rat ovarian surface epithelial cells in vitro. Endocrine 2000;12: 295–302
65. Yu X, Miyamoto S, Mekada E. Integrin alpha 2 beta 1-dependent EGF receptor activation at cell-cell contact sites. J Cell Sci 2000;113:2139–47
66. Cappello S, Attardo A, Wu X, et al. The Rho-GTPase cdc42 regulates neural progenitor fate at the apical surface. Nat Neurosci 2006;9:1099–107
67. Costa MR, Wen G, Lepier A, et al. Par-complex proteins promote proliferative progenitor divisions in the developing mouse cerebral cortex. Development 2008;135:11–22
68. Klezovitch O, Fernandez TE, Tapscott SJ, et al. Loss of cell polarity causes severe brain dysplasia in Lgl1 knockout mice. Genes Dev 2004; 18:559–71
69. Nechiporuk T, Fernandez TE, Vasioukhin V. Failure of epithelial tube maintenance causes hydrocephalus and renal cysts in Dlg5$^{-/-}$ mice. Dev Cell 2007;13:338–50
70. Rodriguez EM, Guerra MM, Vio K, et al. A cell junction pathology of neural stem cells leads to abnormal neurogenesis and hydrocephalus. Biol Res 2012;45:231–42
71. Gotz M, Huttner WB. The cell biology of neurogenesis. Nat Rev Mol Cell Biol 2005;6:777–88
72. Sarnat HB. Regional differentiation of the human fetal ependyma: Immunocytochemical markers. J Neuropathol Exp Neurol 1992;51:58–75
73. Yung YC, Mutoh T, Lin ME, et al. Lysophosphatidic acid signaling may initiate fetal hydrocephalus. Sci Transl Med 2011;3:99ra87